ERJ Express. Published on March 28, 2007 as doi: 10.1183/09031936.00138206

The TGF-β/Smad2,3 signalling axis is impaired in experimental pulmonary hypertension

Anna Zakrzewicz, Fotini M. Kouri, Bozena Nejman, Grazyna Kwapiszewska, Matthias Hecker, Roxana Sandu, Eva Dony, Werner Seeger, Ralph T. Schermuly, Oliver Eickelberg, and Rory E. Morty

Department of Internal Medicine, University of Giessen Lung Center, Justus Liebig University, Giessen, Germany

Address correspondence to: Rory E. Morty
Department of Internal Medicine
University of Giessen Lung Center, Justus Liebig University
Aulweg 123 (Raum 6-11), D-35392 Giessen
Germany
Tel: +49 641 994 7191
Fax: +49 641 994 2308
e-mail: rory.morty@innere.med.uni-giessen.de

Running title: TGF-β signalling in monocrotaline-induced PAH

Support Statement: The authors are supported by the Deutsche Forschungsgemeinschaft (SFB547 "Cardiopulmonary Circulation"), the "Excellence Cluster Cardiopulmonary System" of the universities of Giessen and Frankfurt and the Max Planck Institute for Heart and Lung Research in Bad Nauheim, and the European Commission Sixth European Framework Programme "Pulmotension".

Word-count (Introduction to end of Discussion): 3439

ABSTRACT: Mutations in genes encoding members of the transforming growth factor (TGF)-β superfamily have been identified in idiopathic forms of pulmonary arterial hypertension (PAH). We asked whether perturbations to the TGF-β/Smad2,3 signalling axis occurred in a monocrotaline (MCT) rodent model of experimental PAH.

Expression of the TGF-β signalling machinery was assessed in the lungs and kidneys of MCT-treated rodents with severe PAH, by semi-quantitative reverse-transcription polymerase chain reaction (RT-PCR), real-time RT-PCR, and immunoblot. TGF-β signalling was assessed in the lungs and in pulmonary artery smooth muscle cells (PASMC) from MCT-treated rodents by Smad2 phosphorylation, expression of the *ctgf* gene, activation of the *serpine* promoter in a luciferase reporter system, and by the induction of apoptosis.

The expression of Acvrl1 (a type I TGF-β receptor), Tgfbr2 (the type II TGF-β receptor), endoglin (a type III TGF-β receptor), Smad3 and Smad4; as well as TGF-β signalling and TGF-β-induced apoptosis, were dramatically reduced in the lungs and PASMC, but not the kidneys, of MCT-treated rodents that developed severe PAH.

Our data indicate that the TGF-β/Smad2,3 signalling axis is functionally impaired in MCT-treated rodents with severe PAH, underscoring the potential importance of TGF-β/Smad2,3 signalling in the onset or development of PAH.

Key words: apoptosis; monocrotaline; pulmonary artery smooth muscle cell; transforming growth factor-beta; vascular remodelling

INTRODUCTION

Pulmonary vasoconstriction, vascular remodelling and thrombosis are the underlying causes of increased pulmonary vascular resistance, and thus the elevated pulmonary artery pressure, observed in patients with pulmonary arterial hypertension (PAH) [1, 2]. The vascular remodelling observed in small, normally non-muscularised, pulmonary arteries involves an increase in pulmonary artery smooth muscle cell (PASMC) mass, secondary to endothelial dysfunction. Together, these changes result in medial hypertrophy, concentric obliteration of the lumina, and the formation of complex vascular structures known as plexiform lesions [3].

Although PAH can be inherited (familial PAH; FPAH) or occur sporadically (idiopathic PAH; IPAH) [4], the pathophysiological mechanisms at play during vascular remodelling in PAH have not been identified. Candidate effector molecules include serotonin, angiopoietin, and also bone morphogenetic proteins (BMPs), which form a branch of the transforming growth factor (TGF)-β superfamily of growth factors [1, 2]. Mutations in the gene encoding the type II BMP receptor are considered, at least in part, to be the genetic basis of FPAH, and BMP signalling has consequently received much attention in this context [1, 2, 5]. In contrast, signalling by the TGF-β branch of this superfamily of growth factors has received comparatively little attention [6].

TGF-β signalling is initiated by binding of TGF-β ligand to the type II TGF-β receptor (Tgfbr2, also called TβRII) [7]. This promotes complex formation with one of two type I TGF-β receptors, either Tgfbr1 [activin-like kinase (ALK)-5] or Acvrl1 (ALK-1) [7]. Complex formation may be assisted by accessory type III TGF-β receptors, either Tgfbr3 (betaglycan) or endoglin (the *eng* gene product, CD105). Signals are transmitted by intracellular signalling Smad molecules, notably Smads 2, 3 and 4 [7], and TGF-β signalling may be antagonised by the inhibitory Smads, Smad6 and Smad7 [7].

Mutations and polymorphisms in genes encoding TGF-β signalling machinery, and their functional consequences, have been implicated in many lung pathologies, including sarcoidosis [8] and chronic obstructive pulmonary disease [9]. With respect to PAH, mutations have been identified in *eng* [10] and *acrvl1* [11, 12] genes in patients with hereditary haemorrhagic telangiectasia and coexistent PAH, as well as in children with IPAH [13]. Somatic mutations in *tgfbr2* have been reported in endothelial cells within plexiform lesions of IPAH patients [14]. Therefore, mutations in all three types of TGF-β receptors have been described in PAH. Furthermore, reduced expression of genes encoding TGF-β3 and Tgfbr3 has been demonstrated in IPAH patients [15]. Endothelial cells of plexiform lesions in IPAH patients exhibit reduced expression of TGF-β receptors and Smad proteins [6], and dysregulated TGF-β signalling is observed in pulmonary artery smooth muscle cells (PASMC), where TGF-β promoted the proliferation of PASMC from IPAH patients [16], but exhibited an opposite (growth inhibitory) effect on PASMC from healthy donors [16, 17]. Together, these data overwhelmingly implicate dysregulated TGF-β signalling in PAH, although no study to date has examined TGF-β/Smad signalling in an animal model of PAH. In this study, we set out to investigate whether perturbations to the TGF-β/Smad2 signalling axis occurred during monocrotaline-induced pulmonary hypertension, a popular but poorly understood animal model for human PAH.

MATERIALS AND METHODS

Animals and haemodynamics **-** The animal ethics authority of the government of the State of Hessen approved all animal procedures. Pulmonary hypertension was induced in adult male Sprague-Dawley rats by a single intraperitoneal injection of MCT (60 $mg.kg^{-1}$; Sigma, St. Louis, USA). Haemodynamic measurements and lung extraction were performed as described previously [18].

RNA isolation, semi-quantitative and real-time polymerase chain reaction **-** Total RNA was isolated from fresh lung tissue using a Qiagen RNeasy kit (Qiagen, Hilden, Germany), and screened by semi-quantitative reverse transcription (RT) polymerase chain reaction (PCR) [19] using the intron-spanning primers indicated in table 1. Cycle numbers lie in the logarithmic phase for each PCR. Quantitative changes in gene expression were also analysed by real-time RT-PCR by the $\Delta\Delta C_t$ method [20], using the primer pairs indicated in table 1, and the hydroxymethylbilane synthase (*hmbg*) gene as reference.

Protein isolation and immunoblotting **-** Protein extraction, gel electrophoresis and immunoblotting were performed as described previously [19, 21]. Blots were probed with antibodies to Acvrl1 (1 $\mu g.ml^{-1}$; R&D Systems, Minneapolis, USA), Tgfbr1 (1:1500) and Tgfbr2 (1:1000; Santa Cruz, San Fransisco, USA), phospho-Smad2(Ser465/467), Smad3 and Smad4 (all 1:1000; Upstate, Charlottesville, USA), Smad2 (1:1000; Zymed, San Fransisco, USA), and β-actin (1:1000; Cell Signaling Technology, Danvers, USA). Peroxidase-conjugated secondary antibodies were from R&D Systems (Wiesbaden, Germany).

Immunohistochemistry **-** Elastin and H&E staining, and immunofluorescence was performed on 3 μm tissue sections [18], with antibodies against smooth muscle actin (SMA; 1:850; Sigma, Taufkirchen, Germany), von Willebrand factor (1:800; Dako, Hamburg, Germany); Tgfbr1 (R-20), Tgfbr2 (H-567) and proliferating cell nuclear antigen (PCNA; all at 1:100; Santa Cruz, San Fransisco, USA), Smad3 and Smad4 (both at 1:50; Upstate, Charlottesville, VA), Smad2 (R&D Systems, Minneapolis, USA), and phospho-Smad2 (Cell Signaling Technology, Danvers, USA). Immune-complexes were visualised with a Histostain *Plus* Kit (Zymed, San Fransisco, USA). Immunohistochmemistry was quantified by counting the number of positive cells as a percentage of the total number of cells counted. It is important to stress that those data reflect absolute changes (positive *versus* negative staining) in a signal, and do not reflect intermediate changes (strong *versus* weak staining) in signal intensity; therefore, data must be interpreted with caution.

Luciferase reporter assay **-** Primary rat PASMC were isolated from the second to the fifth branch of the pulmonary artery as described previously [18] from saline-treated control or MCT-treated rats. Early passage (first two passages) PASMC, seeded in 24-well plates (70% confluent), were transiently transfected with LipofectAMINE (Invitrogen, Karlsruhe, Germany) as described for human PASMC [22], with $p(CAGA)_{12}$-luc, a reporter construct that contains a TGF-β-responsive promoter derived from the *serpine1* gene, located upstream of a firefly luciferase gene [23]. Alternatively, cells were transfected with pGL3-Basic (containing a promoterless luciferase gene) or pGL3-Control (containing a constitutively-expressed luciferase gene) both from Promega (Mannheim, Germany) as negative and positive controls, respectively. Cells were incubated with TGF-β1 (R&D Systems, Wiesbaden, Germany; 2 $ng.ml^{-1}$) for 12 h, firefly luciferase activity assessed [19]. Values were normalised for the transcriptional activity of the pGL3-control vector.

Assessment of apoptosis of PASMC - Early passage PASMC were seeded at 1×10^4 cells/well in chamber slides and grown to ≈80% confluence. Quiescent cells [cultured in 0.1 % (v/v) FBS for 48 h] were treated with TGF-β1 (2 $ng.ml^{-1}$; 24 h) and apoptosis assessed using a terminal deoxyribonucleotidyl transferase-mediated deoxyuridine triphosphate nick end-labelling (TUNEL) assay (Roche, Indianapolis, USA) [18]. Cells were scored for TUNEL and 4′,6′-diamino-2-phenylindole staining in twenty random fields per sample.

Statistical treatment of data **-** Data are presented as mean ± S.D. Differences between groups were analysed by ANOVA and the Student-Newman-Keul *post-hoc* test for multiple comparisons, with a P value < 0.05 regarded as significant.

RESULTS

MCT causes severe PAH and vascular remodelling in rats

Administration of MCT caused pronounced vascular remodelling and PAH in rats four weeks after administration. Vascular remodelling was evident by thickening of the vessel walls of the small pulmonary arteries (fig. 1a-d), together with a significant 44% increase in the right ventricle-to-left ventricle+septum ratio (table 2), indicative of right heart hypertrophy. These changes were accompanied by a two-fold increase in right ventricular systolic pressure (table 2) indicative of severe PAH, and a 30% decrease in the partial pressure of oxygen in arterial blood (table 2), although no significant change (11% reduction) in systemic arterial pressure was observed (table 2).

Expression of TGF-β signalling machinery is reduced in the lungs of MCT-treated rats

A dramatic decrease in expression of mRNA encoding Tgfbr2, endoglin, Acvrl1, Smad3 and Smad4 was observed by real-time RT-PCR in the lungs of rats four weeks after MCT treatment (fig. 1e). Similarly, downregulated expression of genes encoding Tgfbr2, Avcrl1, Smad3 and Smad4 was observed in lungs, but not kidneys, of rats four weeks after MCT administration, by semi-quantitative RT-PCR (fig. 1f). The mRNA levels of the endothelial markers *pecam1* and *vwf* were unaltered at two and four weeks post-MCT treatment (fig. 1e), indicating no major loss of endothelium at these time-points. We employed the *hmox1* gene as a control, since its expression is elevated in the lungs of MCT-treated rats that develop PAH [24].

Since changes in mRNA expression do not always reflect changes in the protein expression [25], we also assessed protein expression by immunoblot. Consistent with our RT-PCR data, significantly reduced levels of Tgfbr2, Avcrl1, Smad3 and Smad4 were observed in the lungs of MCT-treated rats four weeks after MCT administration (fig. 2).

Antibodies against Acvrl1 did not yield any signal over background staining on lung sections (data not shown). However, both Tgfbr1 and Tgfbr2 exhibited strong staining in the airway epithelium in saline-treated rats (fig. 3a-b, e-f). Staining for Tgfbr1 was also evident in the smooth muscle and endothelium of saline-treated rats (fig. 3a-b). In the case of Tgfbr1, the staining exhibited similar intensity and pattern in MCT-treated rats, although the background was higher due to intense inflammtory cell infiltration (figs 3c-d, 4a). However, staining for Tgfbr2 was noticeably weaker in the airway epithelial layer (fig. 3g-h), and tended towards reduced levels in the vascular smooth muscle layer of small vessels of MCT-treated rats (fig. 4a). These data are consistent with our observations that mRNA and protein expression of Tgfbr1 and Tgfbr2 are reduced the lungs of MCT-treated rats.

In the case of Smad proteins, staining for Smad2 was strong, particularly in the airway epithelium of both saline- and MCT-treated rats (figs 3j-l, 4a). In contrast, while intense staining for Smad3 and Smad4 in the airway epithelium was observed for saline-treated rats (figs 3m-n, q-r; 4a), this staining was markedly reduced in MCT-treated rats (figs 3o-p, s-t; 4a). Of interest, Smad4 exhibited a strong nuclear staining in the endothelium of saline-treated rats (fig. 3s, *inset*), in approximately 77 ± 6 % of cells counted, while this staining was largely lost in MCT-treated rats (8 ± 4 % of cells counted). Similarly, Smad4 staining exhibited a reduced trend in the vascular smooth muscle of MCT-treated rats (fig. 4a), however, this trend did not approach statistical significance. These data support our observations that the mRNA and proteins levels of Smad3 and Smad4 are reduced in MCT-treated rats.

The TGF-β/Smad2,3 signalling axis is impaired in the lungs of MCT-treated rats

Our observations that MCT administration caused a dramatic reduction in the expression of TGF-β receptors and Smads, suggested to us that TGF-β signalling would be perturbed in the lungs of MCT-treated rats. Indeed, while phospho-Smad2 staining was evident in the vascular

smooth muscle and airway epithelium of lungs from saline-treated rats, this staining was largely lost in lungs from MCT-treated rats (fig. 4b). Furthermore, baseline levels of phospho-Smad2 (although not total Smad2 levels) were significantly reduced in whole lung extracts from MCT-treated rats (fig. 4c, e) suggesting functional impairment of the TGF-β/Smad2,3 signalling axis. Interestingly, this decrease was evident before changes in TGF-β receptor or Smad expression were evident by immunoblot (fig. 2a), suggesting other mechanisms at play that downregulate TGF-β/Smad2 signalling (perhaps in response to the massive inflammation in lungs at two weeks post-MCT adminsitration), or that the receptor and Smad expression changes were too subtle to be evident by immunoblot at this time-point.

Together, these data suggest that the expression of TGF-β-induced genes in the lung would also be down-regulated. To test this idea, we examined mRNA levels encoding the *ctgf* gene, which is a TGF-β-regulated gene that encodes connective tissue growth factor (CTGF). As expected, the *ctgf* mRNA levels were significantly lower in the lungs of MCT-treated rats, although not in the kidneys (fig. 4d, f). Our data therefore indicate that MCT administration specifically perturbs TGF-β signalling in the lungs of rats in this experimental model of PAH.

Given the important growth-regulatory roles of TGF-β, we also assessed cell proliferation in lungs from MCT-treated rats by staining for PCNA. Few proliferating cells were evident in lungs of saline-treated rats (fig. 5a, d). However, two-weeks after MCT administration, increased cell proliferation was observed in the alveolar septae, smooth muscle and endothelium of the lung (fig. 5b, e). Additionally, massive inflammatory cell infiltration was evident two weeks post-MCT administration, evident from a dramatically increased number of macrophages (*arrows*, fig. 5b). Four weeks after MCT administration, proliferating cells were detected primarily in the smooth muscle layer of pulmonary arteries, although proliferating cells were also evident in the airway epithelium and the interstitium (fig. 5c, f).

The TGF-β/Smad2,3 signalling axis is impaired in PASMC from MCT-treated rats

Our data thus far have relied on experiments in whole lung homogenates, which reflect the net TGF-β signalling capacity of the endothelium, epithelium, smooth muscle, and fibroblast and inflammatory cell composition of the lung. We felt it relevant to examine TGF-β signalling in a single cell type. Since PASMC (which are responsive to TGF-β [16, 17]) are accredited with a key role in the pathogenesis of familial and non-familial forms of PAH [1], and we observe increased PASMC proliferation in the lungs of rats after MCT treatement, we examined TGF-β signalling in PASMC isolated from the lungs of saline- or MCT-treated rats (fig. 5).

Baseline phospho-Smad2 levels (but not total Smad2 levels) were reduced in PASMC from MCT-treated rats, indicating that the TGF-β/Smad2 axis was also functionally impaired in PASMC. Specific induction of TGF-β signalling was investigated by transfecting the p$(CAGA)_{12}$-luc reporter plasmid [23] into PASMC derived from saline- or MCT-treated rats. This plasmid contains a firefly luciferase gene, located downstream of a TGF-β responsive promoter derived from the *serpine1* gene. The induction of luciferase activity by TGF-β is therefore a measure of TGF-β signalling. The ability of TGF-β to induce luciferase expression was markedly (two-fold) lower in PASMC from MCT treated rats (fig. 5b), confirming that the TGF-β/Smad axis is functionally impaired in PASMC from MCT-treated rats.

Since TGF-β can induce apoptosis in PASMC [17], we reasoned that this effect would be less apparent in PASMC from MCT-treated rats. Indeed, a more than two-fold reduction in the induction of apoptosis by TGF-β was observed in PASMC from MCT-treated rats, as assessed by TUNEL staining. These data indicate that functional impairment of the TGF-β/Smad signalling axis in PASMC from MCT-treated rats is physiologically relevant. This idea is supported by the increased PASMC proliferation in the lungs of MCT-treated rats we report here (PCNA staining; fig. 5), and the complete absence of apoptosis in PASMC noted in MCT-treated rats in another study [18].

DISCUSSION

A growing body of evidence points to a key role for dysregulated signalling by the BMP/Smad1,5,8 axis of the TGF-β growth factor superfamily in the onset or development of PAH [1, 2, 4, 6, 12-16]. In contrast, a role for the TGF-β/Smad2,3 axis in PAH has been relatively unexplored. Therefore, the aim of this study was to establish whether the TGF-β/Smad signalling axis was impaired in MCT-induced PAH in rats, a popularly used, albeit poorly understood model for familial and idiopathic PAH.

We document here a dramatic down-regulation of expression of both TGF-β receptors, and some of their associated Smad proteins, four weeks after MCT administration, by which time pronounced pulmonary vascular remodelling and PAH were evident. Amongst the receptors, a dramatic decrease in Acvrl1 and Tgfbr2 expression was evident, while expression of Tgfbr1 was unchanged. Similarly, expression of two key TGF-β intracellular signalling molecules, Smad3 and Smad4, was decreased. These changes were restricted to the lung, since they were not observed in the kidneys of MCT-treated rats. Furthermore, levels of both phosphorylated Smad2 and of mRNA encoding CTGF were also down-regulated, indicating diminished TGF-β signalling in the lungs, but not the kidneys, of MCT-treated rats with severe PAH. In PASMC isolated from MCT-treated rats, both baseline and induced TGF-β signalling were also reduced, compared with PASMC from saline-treated controls. This impaired TGF-β signalling was physiologically relevant, since PASMC from MCT-treated rats were resistant to the pro-apoptotic effects of TGF-β. Taken together, our data demonstrate dramatically impaired signalling by the TGF-β/Smad axis in the lungs of MCT-treated rats with severe PAH.

Four-fold elevated levels of TGF-β have been described during MCT-induced PAH in rats [26], and it has been suggested that this may underlie the increased expression of some

extracellular matrix genes in this model. Our data would argue that this is not the case, but rather that the two-fold increase in mRNA encoding tropoelastin, fibronectin and collagen Iα_1 levels observed in that study may have been induced by other fibrogenic cytokines, possibly interleukin 1α and β, and tumour necrosis factor-α, since levels of all three cytokines are elevated in MCT-induced PAH. Interestingly, induction of a dominant-negative Tgfbr2 gene in hypoxia-induced PAH attenuated hypoxia-driven vascular remodelling and pulmonary hypertension [27]. Those data suggest a protective role for Tgfbr2 in hypoxia-driven PAH, in contrast to our data, which correlate reduced Tgfbr2 with increased abberant vascular remodelling in MCT-induced PAH. Together, these data emphasise that the vascular remodelling in these two models is very different [28], an idea underscored by the recent observation that bone marrow-derived progenitor cells can limit pulmonary vascular remodelling induced by MCT, but not that induced by hypoxia [29].

A common feature of the vascular remodelling observed in all forms of PAH is the increased muscularisation of small pulmonary arteries [1, 2]. This has, in part, been attributed to the aberrant growth of PASMC, which exhibit impaired responses to stimuli that control proliferation and apoptosis of PASMC. TGF-β is one of those stimuli, promoting the apoptosis of healthy PASMC [17] and inhibiting the proliferation of healthy PASMC, and PASMC from patients with Eisenmenger's syndrome who exhibit PAH secondary to ventricular septal defects [16]. However, PASMC from patients with IPAH or FPAH are resistant to the anti-proliferative effects of TGF-β [16], suggesting that the failure of TGF-β to control PASMC growth in PAH may, in part, underlie the increased muscularisation of normally non-muscularised small pulmonary arteries of patients with FPAH or IPAH. Data we present in the present manuscript support this idea, since increased muscularisation of small pulmonary arteries was also observed in MCT-treated rats with severe PAH, and PASMC from these rats

were insensitive to the pro-apoptotic effects of TGF-β. Thus, impaired TGF-β signaling in PASMC appears to be a common feature of human IPAH and MCT-induced PAH.

In addition to PASMC, dysregulated TGF-β signalling is also likely to impact the endothelium. Endothelial cells are peculiar in that they express two different type I TGF-β receptors: Tgfbr1 and Acvrl1. These two receptors mediate opposing effects by TGF-β on endothelial function, and together they balance the activation state of the endothelium. Signalling by Acvrl1 promotes endothelial cell proliferation and migration [30], and endoglin plays a key role in promoting these effects [31], thereby stimulating angiogenesis. In contrast, signalling by Tgfbr1 opposes Acvrl1/endoglin signalling, and inhibits endothelial cell proliferation and migration, and maintains the endothelium in a quiescent state [30]. We present data in this report that demonstrated a significant down-regulation of *both* Acvrl1 and endoglin expression in the lungs of MCT-treated rats, while Tbgbr1 expression remained unchanged. These data suggest that, in the context of TGF-β signalling, the balance is tipped strongly in favour of Tgfbr1 signalling, which would maintain a quiescent endothelium in MCT-induced PAH. This idea is supported by the observation that MCT has a cytostatic effect on the rat pulmonary endothelium [32]. Clearly, however, this idea remains speculative since we have not examined isolated endothelial cells in this study.

The data we present here support a role for reduced TGF-β signalling in promoting PAH. This idea gains credence from observations that the converse situation, that is, *increased* TGF-β signalling, can afford protection *against* PAH. For example, in patients with very severe (GOLD stage IV) COPD, the expression of Smads 2,3 and 4 was normal, while that of the inhibitory Smad, Smad7, was reduced [33], which would lead to potentiated TGF-β signalling. In a separate study it was demonstrated that expression of Tgfbr2 was up-regulated in the pulmonary arteries of patients with very severe COPD [34]. Together, these studies suggested that TGF-β signalling is increased in COPD, leading Beghe *et al.* [34] to propose

that up-regulation of TGF-β signalling in severe COPD has a protective (anti-proliferative) role, perhaps explaining the low incidence of severe pulmonary hypertension seen in COPD patients [35].

In sum, our data suggest that dramatically reduced expression of components of the TGF-β signalling machinery results in impaired TGF-β signalling in the lungs of MCT-treated rats. This dysregulated TGF-β signalling may underlie the aberrant proliferation of PASMC seen in MCT-induced PAH; and also has implications for the activation state of the endothelium. Our data strongly support a role for impaired TGF-β signalling in the onset and developments of sporadic and familial forms of IPAH, in which germline mutations in genes encoding the TGF-β signalling machinery have already been reported.

REFERENCES

1. Humbert, M., N. W. Morrell, S. L. Archer, K. R. Stenmark, M. R. MacLean, I. M. Lang, B. W. Christman, E. K. Weir, O. Eickelberg, N. F. Voelkel, and M. Rabinovitch. Cellular and molecular pathobiology of pulmonary arterial hypertension. *J Am Coll Cardiol* 2004; 43: 13S-24S.

2. Eddahibi, S., N. Morrell, M. P. d'Ortho, R. Naeije, and S. Adnot. Pathobiology of pulmonary arterial hypertension. *Eur Respir J* 2002; 20: 1559-1572.

3. Voelkel, N. F., and R. M. Tuder. Cellular and molecular mechanisms in the pathogenesis of severe pulmonary hypertension. *Eur Respir J* 1995; 8: 2129-2138.

4. Rubin, L. J. Primary pulmonary hypertension. *N Engl J Med* 1997; 336: 111-117.

5. Dinh-Xuan, A. T., M. Humbert, and R. Naeije. Severe pulmonary hypertension: walking through new paths to revisit an old field. *Eur Respir J* 2002; 20: 509-510.

6. Richter, A., M. E. Yeager, A. Zaiman, C. D. Cool, N. F. Voelkel, and R. M. Tuder. Impaired transforming growth factor-beta signaling in idiopathic pulmonary arterial hypertension. *Am J Respir Crit Care Med* 2004; 170: 1340-1348.

7. Massagué, J. TGF-beta signal transduction. *Annu Rev Biochem* 1998; 67: 753-791.

8. Murakozy, G., K. I. Gaede, G. Zissel, M. Schlaak, and J. Müller-Quernheim. Analysis of gene polymorphisms in interleukin-10 and transforming growth factor-beta 1 in sarcoidosis. *Sarcoidosis Vasc Diffuse Lung Dis* 2001; 18: 165-169.

9. Wu, L., J. Chau, R. P. Young, V. Pokorny, G. D. Mills, R. Hopkins, L. McLean, and P. N. Black. Transforming growth factor-beta1 genotype and susceptibility to chronic obstructive pulmonary disease. *Thorax* 2004; 59: 126-129.

10. Chaouat, A., F. Coulet, C. Favre, G. Simonneau, E. Weitzenblum, F. Soubrier, and M. Humbert. Endoglin germline mutation in a patient with hereditary haemorrhagic

telangiectasia and dexfenfluramine associated pulmonary arterial hypertension. *Thorax* 2004; 59: 446-448.

11. Harrison, R. E., J. A. Flanagan, M. Sankelo, S. A. Abdalla, J. Rowell, R. D. Machado, C. G. Elliott, I. M. Robbins, H. Olschewski, V. McLaughlin, E. Gruenig, F. Kermeen, M. Halme, A. Raisanen-Sokolowski, T. Laitinen, N. W. Morrell, and R. C. Trembath. Molecular and functional analysis identifies ALK-1 as the predominant cause of pulmonary hypertension related to hereditary haemorrhagic telangiectasia. *J Med Genet* 2003; 40: 865-871.

12. Trembath, R. C., J. R. Thomson, R. D. Machado, N. V. Morgan, C. Atkinson, I. Winship, G. Simonneau, N. Galie, J. E. Loyd, M. Humbert, W. C. Nichols, N. W. Morrell, J. Berg, A. Manes, J. McGaughran, M. Pauciulo, and L. Wheeler. Clinical and molecular genetic features of pulmonary hypertension in patients with hereditary hemorrhagic telangiectasia. *N Engl J Med* 2001; 345: 325-334.

13. Harrison, R. E., R. Berger, S. G. Haworth, R. Tulloh, C. J. Mache, N. W. Morrell, M. A. Aldred, and R. C. Trembath. Transforming growth factor-beta receptor mutations and pulmonary arterial hypertension in childhood. *Circulation* 2005; 111: 435-441.

14. Yeager, M. E., H. A. Golpon, N. F. Voelkel, and R. M. Tuder. Microsatellite mutational analysis of endothelial cells within plexiform lesions from patients with familial, pediatric, and sporadic pulmonary hypertension. *Chest* 2002; 121: 61S.

15. Geraci, M. W., M. Moore, T. Gesell, M. E. Yeager, L. Alger, H. Golpon, B. Gao, J. E. Loyd, R. M. Tuder, and N. F. Voelkel. Gene expression patterns in the lungs of patients with primary pulmonary hypertension: a gene microarray analysis. *Circ Res* 2001; 88: 555-562.

16. Morrell, N. W., X. Yang, P. D. Upton, K. B. Jourdan, N. Morgan, K. K. Sheares, and R. C. Trembath. Altered growth responses of pulmonary artery smooth muscle cells from

patients with primary pulmonary hypertension to transforming growth factor-beta(1) and bone morphogenetic proteins. *Circulation* 2001; 104: 790-795.

17. Zhang, S., I. Fantozzi, D. D. Tigno, E. S. Yi, O. Platoshyn, P. A. Thistlethwaite, J. M. Kriett, G. Yung, L. J. Rubin, and J. X. Yuan. Bone morphogenetic proteins induce apoptosis in human pulmonary vascular smooth muscle cells. *Am J Physiol Lung Cell Mol Physiol* 2003; 285: L740-754.

18. Schermuly, R. T., E. Dony, H. A. Ghofrani, S. Pullamsetti, R. Savai, M. Roth, A. Sydykov, Y. J. Lai, N. Weissmann, W. Seeger, and F. Grimminger. Reversal of experimental pulmonary hypertension by PDGF inhibition. *J Clin Invest* 2005; 115: 2811-2821.

19. Alejandre-Alcázar, M. A., G. Kwapiszewska, I. Reiss, O. A. Amarie, L. M. Marsh, J. Sevilla-Pérez, M. Wygrecka, P. Eul, S. Köbrich, M. Hesse, R. T. Schermuly, W. Seeger, O. Eickelberg, and R. E. Morty. Hyperoxia modulates TGF-beta signaling in a mouse model of bronchopulmonary dysplasia. *Am J Physiol Lung Cell Mol Physiol* 2006; *in press*; doi:10.1152/ajplung.00050.2006.

20. Kwapiszewska, G., J. Wilhelm, S. Wolff, I. Laumanns, I. R. Koenig, A. Ziegler, W. Seeger, R. M. Bohle, N. Weissmann, and L. Fink. Expression profiling of laser-microdissected intrapulmonary arteries in hypoxia-induced pulmonary hypertension. *Respir Res* 2005; 6: 109.

21. Vadász, I., R. E. Morty, A. Olschewski, M. Konigshoff, M. G. Kohstall, H. A. Ghofrani, F. Grimminger, and W. Seeger. Thrombin impairs alveolar fluid clearance by promoting endocytosis of Na^+,K^+-ATPase. *Am J Respir Cell Mol Biol* 2005; 33: 343-354.

22. Brevnova, E. E., O. Platoshyn, S. Zhang, and J. X. Yuan. Overexpression of human KCNA5 increases IK V and enhances apoptosis. *Am J Physiol Cell Physiol* 2004; 287: C715-722.

23. Dennler, S., S. Itoh, D. Vivien, P. ten Dijke, S. Huet, and J. M. Gauthier. Direct binding of Smad3 and Smad4 to critical TGF beta-inducible elements in the promoter of human plasminogen activator inhibitor-type 1 gene. *EMBO J* 1998; 17: 3091-3100.

24. Goto, J., K. Ishikawa, K. Kawamura, Y. Watanabe, H. Matumoto, D. Sugawara, and Y. Maruyama. Heme oxygenase-1 reduces murine monocrotaline-induced pulmonary inflammatory responses and resultant right ventricular overload. *Antioxid Redox Signal* 2002; 4: 563-568.

25. White, C. W., K. E. Greene, C. B. Allen, and J. M. Shannon. Elevated expression of surfactant proteins in newborn rats during adaptation to hyperoxia. *Am J Respir Cell Mol Biol* 2001; 25: 51-59.

26. Tanaka, Y., M. L. Bernstein, R. P. Mecham, G. A. Patterson, J. D. Cooper, and M. D. Botney. Site-specific responses to monocrotaline-induced vascular injury: evidence for two distinct mechanisms of remodeling. *Am J Respir Cell Mol Biol* 1996; 15: 390-397.

27. Chen, Y. F., J. A. Feng, P. Li, D. Xing, Y. Zhang, R. Serra, N. Ambalavanan, E. Majid-Hassan, and S. Oparil. Dominant Negative Mutation of the TGF-beta Receptor Blocks Hypoxia-Induced Pulmonary Vascular Remodeling. *J Appl Physiol* 2005.

28. van Suylen, R. J., J. F. Smits, and M. J. Daemen. Pulmonary artery remodeling differs in hypoxia- and monocrotaline-induced pulmonary hypertension. *Am J Respir Crit Care Med* 1998; 157: 1423-1428.

29. Raoul, W., O. Wagner-Ballon, G. Saber, A. Hulin, E. Marcos, S. Giraudier, W. Vainchenker, S. Adnot, S. Eddahibi, and B. Maitre. Effects of bone marrow-derived cells on monocrotaline- and hypoxia-induced pulmonary hypertension in mice. *Respir Res* 2007; 8: 8.

30. Goumans, M. J., G. Valdimarsdottir, S. Itoh, A. Rosendahl, P. Sideras, and P. ten Dijke. Balancing the activation state of the endothelium via two distinct TGF-beta type I receptors. *EMBO J* 2002; 21: 1743-1753.

31. Lebrin, F., M. J. Goumans, L. Jonker, R. L. Carvalho, G. Valdimarsdottir, M. Thorikay, C. Mummery, H. M. Arthur, and P. ten Dijke. Endoglin promotes endothelial cell proliferation and TGF-beta/ALK1 signal transduction. *EMBO J* 2004; 23: 4018-4028.

32. Hoorn, C. M., J. G. Wagner, and R. A. Roth. Effects of monocrotaline pyrrole on cultured rat pulmonary endothelium. *Toxicol Appl Pharmacol* 1993; 120: 281-287.

33. Zandvoort, A., D. S. Postma, M. R. Jonker, J. A. Noordhoek, J. T. Vos, Y. M. van der Geld, and W. Timens. Altered expression of the Smad signalling pathway: implications for COPD pathogenesis. *Eur Respir J* 2006; 28: 533-541.

34. Beghe, B., E. Bazzan, S. Baraldo, F. Calabrese, F. Rea, M. Loy, P. Maestrelli, R. Zuin, L. M. Fabbri, and M. Saetta. Transforming growth factor-beta type II receptor in pulmonary arteries of patients with very severe COPD. *Eur Respir J* 2006; 28: 556-562.

35. Naeije, R. Pulmonary hypertension and right heart failure in chronic obstructive pulmonary disease. *Proc Am Thorac Soc* 2005; 2: 20-22.

FIGURE LEGENDS

FIGURE 1. Monocrotaline induced pulmonary vascular remodelling and changes in expression of the TGF-β signalling machinery. Changes in medial wall thickness (evident by elastin staining; a-b), and vessel muscularisation [visualised by dual-staining for von Willebrand factor (brown) and smooth muscle actin (purple), and counterstaining with haematoxylin; c-d], were investigated in small pulmonary arteries in rats 28 days after saline (a, c) or monocrotaline (a, b) administration. Changes in the expression of genes encoding the TGF-β signalling machinery were assessed in the lungs and kidneys of saline- or monocrotaline-treated rats by (e) by quantitative real-time RT-PCR (black bars, 2 weeks; hatched bars, 4 weeks; relative to saline-treated controls at 4 weeks) and (f) semi-quantitative RT-PCR. Data represent the mean ± S.D. ¶, $p < 0.05$, relative to controls; *, $p < 0.05$, between indicated groups ($n = 4$, per group). MCT, monocrotaline; wk, weeks.

Figure 1

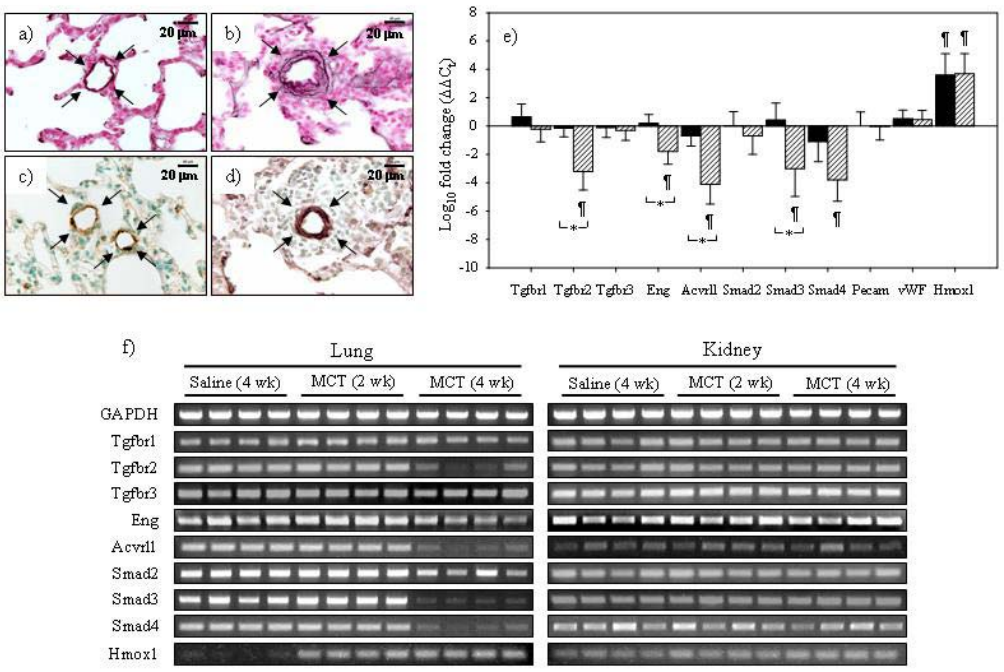

FIGURE 2. Changes in the protein expression of components of the TGF-β signalling machinery in the lungs of monocrotaline-treated rats were assessed by immunoblot (a). Quantitation of immunoblot data is illustrated in (b)-(g). *, $p < 0.05$, relative to controls ($n = 4$, per group). MCT, monocrotaline; wk, weeks.

Figure 2

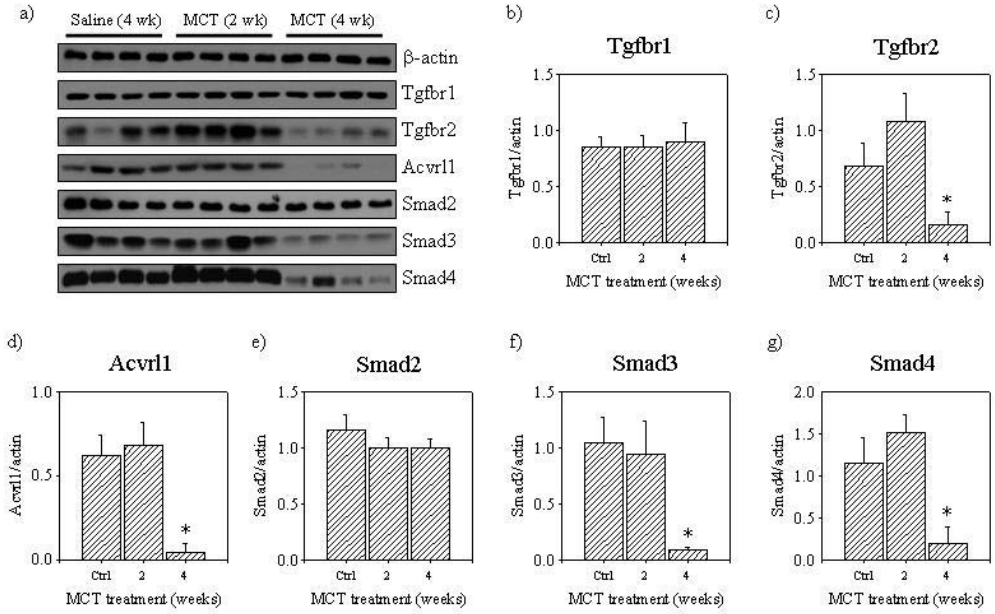

FIGURE 3. Localisation of TGF-β receptors and Smads in lungs from saline- and monocrotaline-treated rats. In the case of vessels, both large (internal diameter 400 - 800 μm) and small (internal diameter 150 - 400 μm; insets) resistance pulmonary arteries are illustrated. a: airways; v: vessels. MCT, monocrotaline.

Figure 3

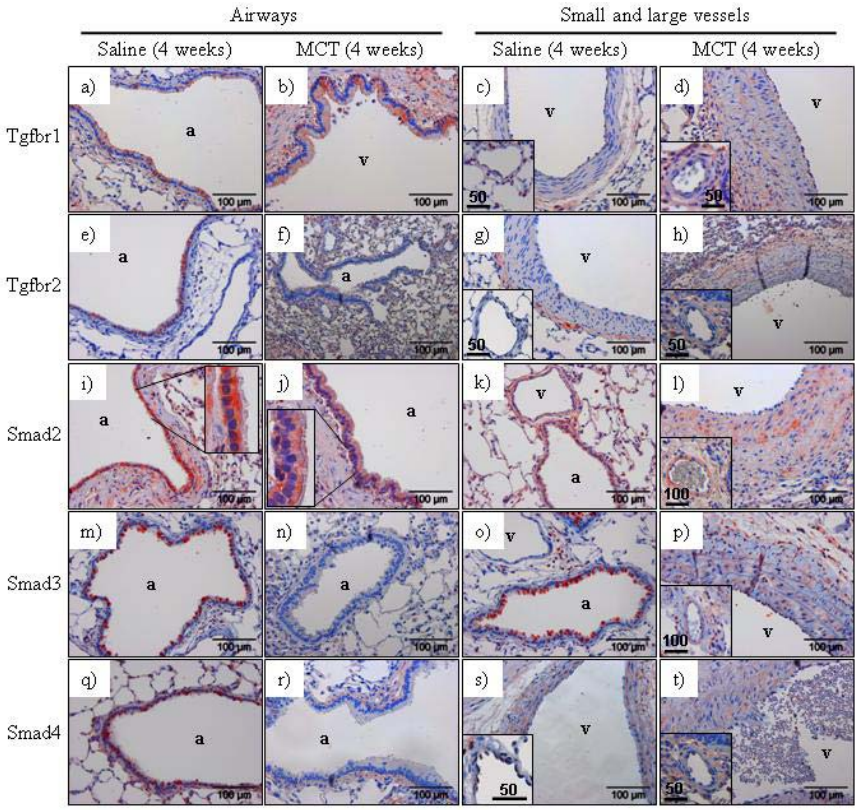

FIGURE 4. Assessment of TGF-β signalling in the lungs of saline- and monocrotaline-treated rats. (a) Expression of TGF-β and Smad proteins was quantitated in the airway epithelium and smooth muscle layer of small vessels in the lungs of saline-treated (black bars) and monocrotaline-treated (hatched bars) rats, four weeks after treatment. Data are presented as the mean number of positive cells ± S.D. in eight representative fields; *, $p < 0.05$, between indicated groups. (b) Localisation of phospho-Smad2 in lungs of saline- and monocrotaline-treated rats. The areas demarcated in the upper two photomicrographs are enlarged in the lower panels. Arrowheads indicate positive staining. (c) TGF-β signalling was assessed in the lungs of saline- and monocrotaline-treated rats by phospho-Smad2 phosphorylation (c) and expression of the *ctgf* gene (d). These data were quantified by densitometry in (e) and (f)

respectively. *, $p < 0.05$, relative to controls (CTRL; *n* = 3-4, per group). MCT, monocrotaline; wk, weeks.

Figure 4

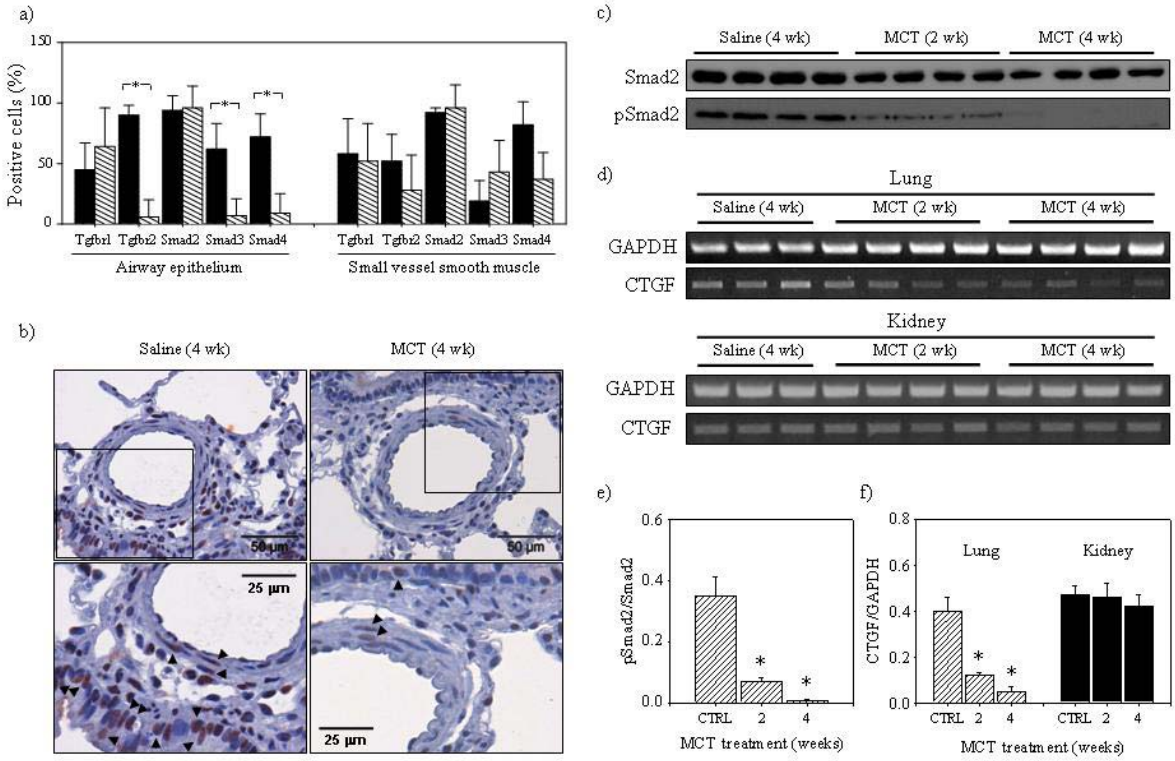

FIGURE 5. Assessment of cell proliferation in the lungs of saline-treated and monocrotaline-treated rats by PCNA staining (red). Areas demarcated in the low magnification photomicrographs in (a), (b) and (c) are magnified in (d), (e) and (f), respectively. Arrowheads indicate positive PCNA staining in the smooth muscle layer of small resistance arteries, while arrows in (b) indicate macrophages. MCT, monocrotaline.

Figure 5

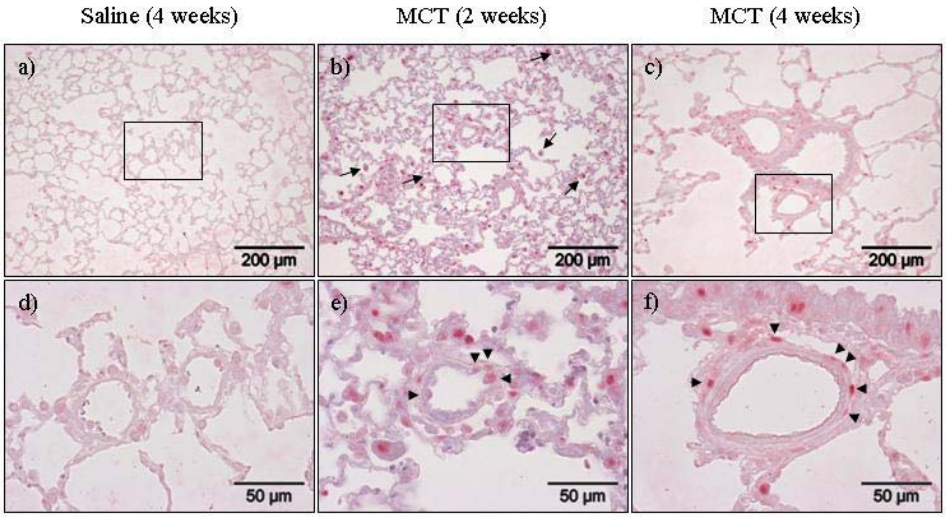

FIGURE 6. TGF-β signalling was impaired in pulmonary artery smooth muscle cells (PASMC) from monocrotaline-treated rats, evident from reduced baseline phospho-Smad2 phosphorylation in non-quiescent cells (a); reduced activity of the TGF-β-responsive element of the *serpine1* promoter in response to TGF-β1 stimulation (b); and in the reduction in number of apoptotic nuclei observed in PASMC from monocrotaline-treated (black bars)) *versus* saline-treated (hatched bars) rats, after TGF-β1 stimulation (c). *, $p < 0.05$, between indicated groups.

Figure 6

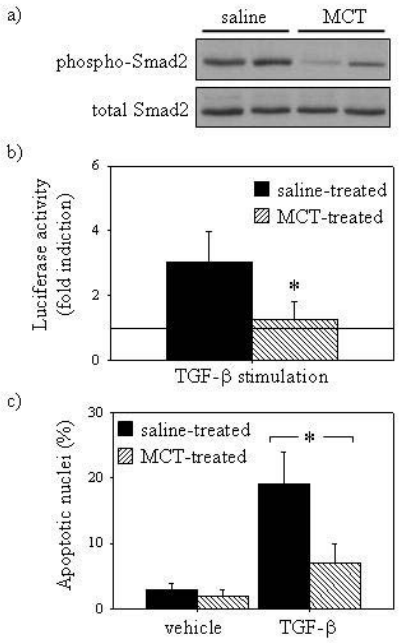
a)
saline
MCT
phospho-Smad2
total Smad2
b)
Luciferase activity (fold indiction)
saline-treated
MCT-treated
*
TGF-β stimulation
c)
Apoptotic nuclei (%)
saline-treated
MCT-treated
*
vehicle
TGF-β

TABLE 1 Primers employed for RT-PCR. Forward and reverse primers are indicated for real-time (rt) and semi-quantitative (sq) PCR reactions.

Gene	Forward Primer	Reverse Primer	Number of cycles	Annealing temperature (ºC)	Amplicon size (bp)
actb (sq)	5′-CTAAGGCCAACCGTGAAAAG-3′	5′-CTTCTGCATCCTGTCAGCAA-3′	20	62.0	611
acvrl1 (sq)	5′-GAGTGTGGCGGTCAAGATTT-3′	5′-TGGTCAACACACACCACCTT-3′	26	59.0	666
avcrl1 (rt)	5′-CCGCACAGACTGTTTTGAGT-3′	5′-TCATAGAAGGGTGGCCTGTA-3′	45	60.0	126
ctgf (rt)	5′-TGCAGCGCGCAGTGTCAGTGC-3′	5′-ACAGTTCTCCCAGCTGCTTGG-3′	45	60.0	112
ctgf (sq)	5′-ATGCTCGCCTCCGTCGCGGGTCC-3′	5′-TGCAGCGCGCAGTGTCAGTGC-3′	28	58.0	1022
eng (rt)	5′-ATGTCTTGGTGAAGCTCCAG-3′	5′-AAAGGATGGTAGTGGTGTGC-3′	45	60.0	100
eng (sq)	5′-ATGACCCCAAAAGCATTGTC-3′	5′-GACGTCATTGCCACACTTTG-3′	27	62.0	605
gapdh (rt)	5′-GAGAATGGGAAGCTGGTCAT-3′	5′-GAAGACGCCAGTAGACTCCA-3′	45	60.0	130
gapdh (sq)	5′-TGGTGAAGGTCGGTGTGAACG-3′	5′-CGCCTGCTTCACCACCTTCTT-3′	22	59.5	788
hmbs (rt)	5′-CCCACGCGAATCACTCTCAT-3′	5′−TGTCTGGTAACGGCAATGCG−3′	45	60.0	118
hmox1 (rt)	5′-CACAGCTCGACAGCATGTCC-3′	5′-ACCCTTCTGAAAGTTCCTCA-3′	45	60.0	110
hmox1 (sq)	5′-TGATGGCCTCCTTGTACCAT-3′	5′-TGCTGATCTGGGATTTTCCT-3′	26	62.5	633
pecam1 (rt)	5′-TGGTACCCGTCCAGGTGTG-3′	5′-GCGGTAAGTGATGGGTGCA-3′	45	60.0	129
smad2 (rt)	5′-TGAGCTTGAGAAAGCCATCA-3′	5′-TGTGTCCCACTGATCTACCG-3′	45	60.0	103
smad2 (sq)	5′-CAGAGGGTGGAGACACCAGT-3′	5′-GCCAGAAGAGCAGCAAATTC-3′	24	59.0	689
smad3 (rt)	5′-CATTACCATCCCCAGGTCAC-3′	5′-CGTAACTCATGGTGGCTGTG-3′	45	60.0	102
smad3 (sq)	5′-CCCCAGAGCAATATTCCAGA-3′	5′-CATCTGGGTGAGGACCTTGT-3′	25	56.0	739
smad4 (rt)	5′-CTCACCCCAGCAAGTGTGTC-3′	5′-CTCCACAGACGGGCATAGAT-3′	45	60.0	116
smad4 (sq)	5′-CCACCAACTTCCCCAACAT-3′	5′-CCAGGACCAGGGATGTTTC-3′	24	57.0	787
tgfbr1 (rt)	5′-CTGCAATCAGGATCACTGCAA-3′	5′-GCAGACTGGACCAGCAATGAC-3′	45	60.0	118
tgfbr1 (sq)	5′-CAAAGGTCGGTTTGGAGAAG-3′	5′-CAACGGATGGATCAGAAGGT-3′	29	55.5	680
tgfbr2 (rt)	5′-GTGAGAAGCCGCAGGAAGTC-3′	5′-CCGTGGTAGGTGAACTTGGG-3′	45	60.0	100
tgfbr2 (sq)	5′-GGGATTGCCATAGCTGTCAT-3′	5′-TGTGAACAATGGGCATCTTG-3′	30	60.5	604
tgfbr3 (rt)	5′-CAGCACCCGGTGTGAACTGT-3′	5′-CTGGCACAGCCAGACAGAAC-3′	45	60.0	90
tgfbr3 (sq)	5′-CCGAGTACCTTCAACCCAAA-3′	5′-CAGTTGAACACTGGGAACGA-3′	29	62.0	668
vwf (rt)	5′-CGGGCGGCTACTGGTTAA-3′	5′-AGGCGTTTCCAAAGTCTACCAC-3′	45	60.0	154

TABLE 2 Induction of pulmonary hypertension in rats by intraperitoneal monocrotaline

	RSVP (mm Hg)	**SAP (mm Hg)**	**RV/LV+S**	**PaO_2 (mm Hg)**
Saline control	29.9 ± 1.8	118.9 ± 23.1	0.30 ± 0.02	202.8 ± 12.9
MCT (2 week)	42.3 ± 12.2	113.6 ± 23.1	0.33 ± 0.05	210.5 ± 38.7
MCT (4 week)	63.5 ± 11.4*	105.5 ± 21.7	0.54 ± 0.09*	143.4 ± 29.0*

Data are presented as mean ± S.D (*n* = 12 animals per group). MCT: monocrotaline; RSVP: right ventricular systolic pressure; RV/LV+S: ratio of right ventricle mass to left ventricle plus septum mass; SAP: systemic arterial pressure; PaO_2: partial pressure of oxygen in arterial blood. *, $P<0.05$ for MCT-treated mice *versus* saline-treated control mice.